

Improved detection of lossy channels by two-mode correlated probes

Carmen Invernizzi* and Matteo G. A. Paris†

Dipartimento di Fisica dell'Università degli Studi di Milano, I-20133 Milano, Italia.

We address the discrimination of lossy channels for continuous variable systems using Gaussian states as probing signals, and focus to the case when one of the values for the loss parameter is zero, i.e. we address the detection of a possible loss against the alternative hypothesis of an ideal lossless channel. We evaluate the quantum Chernoff bound (QCB) and show that optimal probes at fixed energy are given by single- and two-mode squeezed vacuum. We also show that for any value of the damping rate smaller than a critical value there is a threshold on the probe energy that makes two-mode squeezed vacuum more convenient than the corresponding single-mode ones, whereas for damping larger than the threshold two-mode squeezed vacuum are always better than single-mode ones independently on their energy. We then consider discrimination in realistic conditions, where it is unlikely to have pure squeezing, and show that two-mode probes are always better than single-mode ones when all the thermal photons are directed to the dissipative channel. Besides, this result also holds approximately for unbalanced distribution of the thermal photons. We also investigate the role of correlations in the improvement of detection and find that the QCB reduction is a monotone function of the mutual information as well as of entanglement and quantum discord at fixed squeezing. We thus conclude that correlations are a resource for detection of loss independently of their nature, either quantum or classical.

PACS numbers: 42.50.Dv, 42.50.Ex

I. INTRODUCTION

One of the main obstacles to the development of quantum technologies is the decoherence associated to losses and absorption processes occurring during the propagation of a quantum signal. The description of the dynamics of systems subject to noisy environments [1], as well the detection, quantification and estimation of losses and, more generally, the characterization of lossy channels at the quantum level, received much attention in the recent years [1–5]. In this paper we address the discrimination of lossy channels, i.e. we consider a situation where the loss (damping) rate of a channel may assume only two possible values and we want to discriminate between them by probing the channel with a given class of signals. In particular, we address the discrimination of lossy channels for continuous variable systems using Gaussian states as probing signals, and focus attention to the case when one of the values for the loss parameter is zero, i.e. we address the detection of a possible loss against the alternative hypothesis of an ideal lossless channel.

This is a problem of quantum state discrimination and basically consists in looking for the minimum error probability in identifying one of two possible output states from the channel. Upon assuming that repeated probing is possible, i.e. that N identical copies of the output states are given [6–10], the quantity which gives the minimal error probability when discriminating two states is the so-called quantum Chernoff bound (QCB). The use

of QCB in quantum state discrimination is fundamental in several areas of quantum information and it has been exploited as a distinguishability measure between qubits and single-mode Gaussian states [11–13], to evaluate the degree of nonclassicality for one mode Gaussian states [14] or the polarization of a two-mode state [15]. It has also been applied in the theory of quantum phase transitions to distinguish between different phases of the XY model at finite temperature [16], and to the discrimination of two ground states or two thermal states of the quantum Ising model [17].

For continuous variables systems the quantum discrimination of Gaussian states is a central point in view of their experimental accessibility and their relatively simple mathematical description [18, 19]. Upper bounds for the error probability of discrimination of Gaussian states of n bosonic modes have been investigated [13] and closed formula for the QCB of Gaussian states have been derived [11–13].

In this paper, we address the discrimination of lossy channels for continuous variable systems. In particular, our results apply to quantum optical implementations, where single- and two-mode Gaussian states may be reliably realized in a controlled way with current technology [20]. We address the problem of discriminating lossy channels, i.e. we consider that the damping constant of a bosonic channel may be zero or assume a nonzero value, and we want to determine which one on the basis of repeated measurements on the signal exiting the channel. Besides, in order to stay close to schemes feasible with current technology, we analyze in details the effect of the mixedness of probe states. An analogue problem, namely the estimation of the damping constant of a bosonic channel among a continuous set of possible values that it can assume, has already been addressed in literature [21–23],

*Electronic address: Carmen.Invernizzi@unimi.it

†Electronic address: Matteo.Paris@unimi.it

and recently [24] it was proved that two-mode squeezed vacuum probe states are optimal, i.e. they give the best estimate with respect to coherent, thermal or single-mode squeezed states.

The results we report here aim basically at characterizing the kind of states that give the optimal discrimination and whether the improvements obtained in the discrimination using two-mode probes may be ascribed to the correlations between the two modes. To this purpose, besides entanglement and mutual information, we exploit the recent results [25–29] about quantum discord, which has been defined with the aim of capturing quantum correlations in mixed separable states that are not quantified by entanglement.

The paper is structured as follows. In Sec. II we review quantum state discrimination and the definition of quantum Chernoff bound, whereas in Section III we establish notation for Gaussian states and in Section IV we specialize the calculation of the QCB to single- and two-mode Gaussian states. In Sec. V we introduce the discrimination scheme for single-mode and two-mode Gaussian states and calculate the QCB in presence of a lossy channel or an absorber. Section VI reports the main results about the QCB of the single and two-mode states as a function of the total energy for squeezed vacuum probe states or squeezed thermal states. Finally, in Section VII we analyze the role of correlations in the enhancement of the discrimination by two-mode states. Section VIII closes the paper with some concluding remarks.

II. QUANTUM CHERNOFF BOUND

The problem of quantum state discrimination that we consider consists in distinguishing between two possible states, ρ_A and ρ_B which are equiprobable for a quantum system. We suppose that N identical copies of the quantum system are available with the promise that they have been generated either by the source A or B . We can formulate two equiprobable hypotheses H_A and H_B about the identity of the source A, B that has produced the copies, i.e. the global state may be

$$\rho_A^N = \underbrace{\rho_A \otimes \dots \otimes \rho_A}_N \quad \text{or} \quad \rho_B^N = \underbrace{\rho_B \otimes \dots \otimes \rho_B}_N.$$

Then any strategy for the discrimination between these two states amounts to define a two-outcomes POVM $\{E_A, E_B\}$ on the system assigned to each answer H_A, H_B , where $E_A + E_B = \mathbb{I}$ and $E_k \geq 0 \forall k$. After observing the outcome j the observer infers that the state of the system is ρ_j^N . The error probability of inferring the state ρ_j^N when the true state is ρ_k^N is thus given by $P_{jk} = \text{Tr}[\rho_k^N E_j]$ and the optimal POVM for the discrimination problem is the one minimizing the overall probability of a misidentification i.e. $P_e = \frac{1}{2}(P_{BA} + P_{AB})$, where we assumed equiprobable hypotheses. Since $E_A = \mathbb{I} - E_B$,

we have

$$\begin{aligned} P_e &= \frac{1}{2}(\text{Tr}[\rho_A^N E_B]) + \frac{1}{2}\text{Tr}[\rho_B^N E_A] \\ &= \frac{1}{2}(1 - \text{Tr}[E_B \Lambda]) \end{aligned} \quad (1)$$

where we introduced the Helstrom matrix $\Lambda = \rho_B^N - \rho_A^N$. The error probability P_e now has to be minimized over E_B . Since $\text{Tr}[\Lambda] = 0$, the Helstrom matrix has both positive and negative eigenvalues and the minimum P_e is attained if E_B is chosen as the projector over Λ_+ , the positive subspace of Λ . Assuming this optimal operator we have $\text{Tr}[E_B \Lambda] = \text{Tr}[\Lambda_+] = \frac{1}{2} \text{Tr}|\Lambda|$ and $|\Lambda| = \sqrt{\Lambda^\dagger \Lambda}$. Thus the minimal error probability is

$$P_e = \frac{1}{2} \left(1 - \frac{1}{2} \text{Tr}|\rho_A^N - \rho_B^N| \right) \quad (2)$$

The computation of the trace norm of the Helstrom matrix may be rather difficult. For this reason one can resort to the quantum Chernoff bound (QCB) Q that gives an upper bound to the probability of error P_e [11–13]

$$P_e \leq \frac{Q^N}{2} \quad (3)$$

where

$$Q = \min_{0 \leq s \leq 1} \text{Tr}[\rho_A^s \rho_B^{1-s}]. \quad (4)$$

The bound of Eq. (3) is attainable asymptotically in the limit $N \rightarrow \infty$ as follows from the results in [30]. The QCB is a very efficient quantity to be computed and it holds for arbitrary density matrices. Besides, one may think that, though its difficult computation, the trace distance, that is defined as $T(\rho, \sigma) = \frac{1}{2} \text{Tr}|\rho - \sigma|$, has a more natural operational meaning than the QCB. In spite of this, it does not adapt to the case of many copies; indeed, one can find states $\rho, \sigma, \rho', \sigma'$ such that $T(\rho, \sigma) < T(\rho', \sigma')$ but $T(\rho'^N, \sigma'^N) < T(\rho^N, \sigma^N)$. So the QCB does resolve this problem in case of single or many copies of the system.

There is a close relation between Q and the Uhlmann fidelity which is one of the most popular measures of distinguishability for quantum states that is defined as $F(\rho_A, \rho_B) = \text{Tr}[\sqrt{\sqrt{\rho_A} \rho_B \sqrt{\rho_A}}]^2$. As follows from [31], we have that Q gives to P_e a tighter bound than that given from the quantum fidelity:

$$\frac{1 - \sqrt{1 - F(\rho_A, \rho_B)}}{2} \leq P_e \leq \frac{Q}{2} \leq \frac{\sqrt{F(\rho_A, \rho_B)}}{2}.$$

When one of the states is pure, Q equals the fidelity: $Q(\rho_A, \rho_B) = F(\rho_A, \rho_B) = \text{Tr}[\rho_A \rho_B]$.

III. GAUSSIAN STATES

Let us consider an n mode bosonic system described by the tensor product Fock-Hilbert space $\mathcal{H}^{\otimes n}$ and a vector

of quadrature operators $\mathbf{R} = (q_1, p_1, \dots, q_n, p_n)^T$ satisfy the commutation relations

$$[R_j, R_k] = i\Omega_{jk} \quad (5)$$

where Ω_{jk} are the elements of the symplectic matrix

$$\Omega = \bigoplus_{k=1}^n \begin{pmatrix} 0 & 1 \\ -1 & 0 \end{pmatrix}, \quad (6)$$

being $[q_j, p_k] = i\delta_{jk}$, and the mode operators a_k give the canonical operators as follows

$$q_k = \frac{1}{\sqrt{2}}(a_k + a_k^\dagger) \quad p_k = \frac{1}{i\sqrt{2}}(a_k - a_k^\dagger), \quad (7)$$

with commutation relations $[a_j, a_k^\dagger] = \delta_{jk}$. An arbitrary quantum state ρ of the system is fully described by the characteristic function

$$\chi[\rho](\boldsymbol{\lambda}) = \text{Tr}[\rho D(\boldsymbol{\lambda})] \quad (8)$$

where $D(\boldsymbol{\lambda}) = \bigotimes_{k=1}^n D_k(\lambda_k)$ is the n -mode displacement operator, with $\boldsymbol{\lambda} = (\lambda_1, \dots, \lambda_n)^T$, $\lambda_k \in \mathbb{C}$, and $D_k(\lambda_k) = \exp\{\lambda_k a_k^\dagger - \lambda_k^* a_k\}$ is the single mode displacement operator. A state ρ is called Gaussian if the corresponding characteristic function is Gaussian

$$\chi[\rho](\boldsymbol{\Lambda}) = \exp\left\{-\frac{1}{2}\boldsymbol{\Lambda}^T \boldsymbol{\sigma} \boldsymbol{\Lambda} + \mathbf{X}^T \boldsymbol{\Omega} \boldsymbol{\Lambda}\right\} \quad (9)$$

where $\boldsymbol{\Lambda}$ is the real vector $\boldsymbol{\Lambda} = (\text{Re } \lambda_1, \text{Im } \lambda_1, \dots, \text{Re } \lambda_n, \text{Im } \lambda_n)^T$. The covariance matrix $\boldsymbol{\sigma}$ and the vector of mean values \mathbf{X} are defined as

$$X_j = \langle R_j \rangle \\ \sigma_{jk} = \frac{1}{2} \{ \langle R_j, R_k \rangle \} - \langle R_j \rangle \langle R_k \rangle \quad (10)$$

where $\{A, B\} = AB + BA$ denotes the anti-commutator, and $\langle O \rangle = \text{Tr}[\rho O]$ is the mean value of the operator O .

The properties of Gaussian states and operations may be expressed in terms of the covariance matrix and its symplectic transformations. A matrix \mathbf{S} is called symplectic when preserves the symplectic form of Eq. (6), i.e.,

$$\mathbf{S}^T \boldsymbol{\Omega} \mathbf{S} = \boldsymbol{\Omega}. \quad (11)$$

Then, according to the Williamson theorem, for every CM $\boldsymbol{\sigma}$, there exists a symplectic matrix \mathbf{S} such that

$$\boldsymbol{\sigma} = \mathbf{S}^T \mathbf{W} \mathbf{S} \quad (12)$$

where $\mathbf{W} = \bigotimes_{k=1}^n d_k \mathbb{I}_2$ and the d_k 's are the symplectic eigenvalues of $\boldsymbol{\sigma}$. The physical statement implied by decomposition (12) is that every Gaussian state ρ can be obtained from a thermal state ν , described by a diagonal

covariance matrix, by performing the unitary transformation $U_{\mathbf{S}}$ associated to the symplectic matrix \mathbf{S} , i.e.

$$\rho = U_{\mathbf{S}} \nu U_{\mathbf{S}}^\dagger \quad (13)$$

where $\nu = \nu_1 \otimes \dots \otimes \nu_n$ is the tensor product of single-mode thermal states

$$\nu_k = \frac{1}{n_{kT} + 1} \sum_m \left(\frac{n_{kT}}{n_{kT} + 1} \right)^m |m\rangle_{kk} \langle m|$$

with average number of photon given by $n_{kT} = d_k - \frac{1}{2}$.

For a single-mode system the most general Gaussian state may be written as

$$\rho = D(\alpha) S(\zeta) \nu S^\dagger(\zeta) D^\dagger(\alpha) \quad (14)$$

$S(\zeta) = \exp\{\frac{1}{2}(\zeta a^{\dagger 2} - \zeta^* a^2)\}$ being the single-mode squeezing operator and $\alpha, \zeta = r e^{i\phi} \in \mathbb{C}$. The corresponding covariance matrix is given by

$$\boldsymbol{\sigma} = \begin{pmatrix} a & c \\ c & b \end{pmatrix} \quad (15)$$

where

$$a = (n_T + \frac{1}{2}) [\cosh(2r) - \sinh(2r) \cos \phi] \\ b = (n_T + \frac{1}{2}) [\cosh(2r) + \sinh(2r) \cos \phi] \\ c = (n_T + \frac{1}{2}) \sinh(2r) \sin \phi. \quad (16)$$

In the following, for the purposes of channel discrimination, we will consider zero-mean single-mode Gaussian states.

The covariance matrix of a two-mode Gaussian state is a real 4×4 symmetric block matrix. Any two-mode CM $\boldsymbol{\sigma}$ can be recast, upon the action of local symplectic operations, in the standard form [32]

$$\boldsymbol{\sigma} = \frac{1}{2} \begin{pmatrix} A \mathbb{I}_2 & C \sigma_z \\ C \sigma_z & B \mathbb{I}_2 \end{pmatrix} \quad (17)$$

where \mathbb{I}_2 is the 2×2 identity matrix and $\sigma_z = \text{diag}(1, -1)$ the z -Pauli matrix. In the standard form A and B are proportional to the identity matrix and C is diagonal. We assume that also the matrix C is proportional to the identity, i.e., due to their experimental accessibility, we address two-mode squeezed thermal states with a real squeezing parameter r , which corresponds to a CM with parameters

$$A = \cosh(2r) + 2n_{1T} \cosh^2 r + 2n_{2T} \sinh^2 r \\ B = \cosh(2r) + 2n_{1T} \sinh^2 r + 2n_{2T} \cosh^2 r \\ C = (1 + n_{1T} + n_{2T}) \sinh 2r, \quad (18)$$

and density operator $\rho_2 = S_2(r) (\nu_1 \otimes \nu_2) S_2(r)^\dagger$, where $S_2(r) = \exp\{r(a^\dagger b^\dagger - ab)\}$, $r \in \mathbb{R}$ is the two-mode squeezing operator. Using the four local symplectic invariants $I_1 \equiv \det(A \mathbb{I}_2)$, $I_2 \equiv \det(B \mathbb{I}_2)$, $I_3 \equiv \det(C \sigma_z)$ and

$I_4 \equiv \det(\boldsymbol{\sigma})$, the symplectic eigenvalues d_{\pm} can be computed as follows:

$$d_{\pm} = \sqrt{\frac{\Delta(\boldsymbol{\sigma}) \pm \sqrt{\Delta(\boldsymbol{\sigma})^2 - 4I_4}}{2}}, \quad (19)$$

where $\Delta(\boldsymbol{\sigma}) = I_1 + I_2 + 2I_3$.

IV. QUANTUM CHERNOFF BOUND FOR GAUSSIAN STATES

In the following we will focus on single mode and two-mode squeezed thermal states (STS), namely

$$\begin{aligned} \rho_1 &= S(r)\nu S(r)^\dagger \\ \rho_2 &= S_2(r)\nu_1 \otimes \nu_2 S_2(r)^\dagger \end{aligned}$$

As we will see, single- and two-mode STS evolving in a lossy channel lead to a state in the same class and thus the problem of channel discrimination may be reduced to the evaluation of the Chernoff bound for this classes of states. In order to perform this calculation one has to compute the positive power ρ^s . For single mode it can be written as a Gaussian state with a rescaled mean photon number $f(n, s)$, i.e. [13]

$$\rho_1^s = S(r)\nu^s S(r)^\dagger = \mathcal{N}_{(n,s)} S(r)\nu_{(n,s)} S(r)^\dagger \quad (20)$$

where

$$\begin{aligned} \nu^s &= \left(\frac{1}{n+1}\right)^s \sum_{m=0}^{\infty} \left(\frac{n}{n+1}\right)^{ms} |m\rangle\langle m| \\ &= \mathcal{N}_{(n,s)} \frac{1}{f(n,s)+1} \sum_{m=0}^{\infty} \left(\frac{f(n,s)}{f(n,s)+1}\right)^m |m\rangle\langle m| \\ &= \mathcal{N}_{(n,s)} \nu_{(n,s)}, \end{aligned} \quad (21)$$

and

$$\begin{aligned} \mathcal{N}(n,s) &= \text{Tr}[\nu^s] = \frac{1}{(n+1)^s - n^s} \\ f(n,s) &= \frac{n^s}{(n+1)^s - n^s}. \end{aligned} \quad (22)$$

The two mode case follows straightforwardly

$$\begin{aligned} \rho_2^s &= S_2(r)\nu_1^s \otimes \nu_2^s S_2(r)^\dagger \\ &= \mathcal{N}_{(n_1,s)} \mathcal{N}_{(n_2,s)} S_2(r)\nu_{(n_1,s)} \otimes \nu_{(n_2,s)} S_2(r)^\dagger. \end{aligned} \quad (23)$$

We then recall that for any given two squeezed thermal Gaussian states ρ and ρ' , the overlap $\text{Tr}(\rho\rho')$ may be written in terms of their covariance matrices

$$\text{Tr}(\rho\rho') = [\det(\boldsymbol{\sigma} + \boldsymbol{\sigma}')]^{-1/2} \quad (24)$$

where $\boldsymbol{\sigma}, \boldsymbol{\sigma}'$ are the covariance matrices of the two states. Overall, we may write the QCB (4) in the single mode

case $Q_1 = \min Q_{1s}$, where

$$\begin{aligned} Q_{1s} &= \text{Tr} \left[\rho^s \rho'^{(1-s)} \right] \\ &= \mathcal{N}_{(n,s)} \mathcal{N}_{(n',1-s)} \text{Tr} \left[S(r)\nu_{(n,s)} S(r)^\dagger S(r')\nu'_{(n',1-s)} S(r')^\dagger \right] \\ &= \frac{\mathcal{N}_{(n,s)} \mathcal{N}_{(n',1-s)}}{\sqrt{\det(\boldsymbol{\sigma}_{(n,s)} + \boldsymbol{\sigma}'_{(n',1-s)})}}. \end{aligned} \quad (25)$$

For the two-mode case we have $Q_2 = \min Q_{2s}$, where

$$\begin{aligned} Q_{2s} &= \text{Tr} \left[\rho^s \rho'^{(1-s)} \right] \\ &= \frac{\mathcal{N}_{(n_1,s)} \mathcal{N}_{(n_2,s)} \mathcal{N}_{(n'_1,1-s)} \mathcal{N}_{(n'_2,1-s)}}{\sqrt{\det(\boldsymbol{\sigma}_{(n_1,n_2,s)} + \boldsymbol{\sigma}'_{(n'_1,n'_2,1-s)})}}. \end{aligned} \quad (26)$$

V. GAUSSIAN STATES IN A LOSSY CHANNEL

In what follows, we study the evolution of a Gaussian state in a dissipative channel \mathcal{E}_Γ characterized by a damping rate Γ , which may result from the interaction of the system with an external environment, as for example a bath of oscillators, or from an absorption process. We address the problem of detecting whether or not the dissipation dynamics occurred, i.e. the problem of discriminating between an input state ρ and the final state $\rho' = \mathcal{E}_\Gamma(\rho)$. We focus to Gaussian states in view of their experimental accessibility and their relatively simple mathematical description. Besides, lossy channels are Gaussian channels, i.e. transform Gaussian states into Gaussian states.

We assume to have many copies at disposal and thus use the quantum Chernoff bound Q defined in Eq. (4) as a distinguishability measure. A schematic diagram of the measurement schemes we have in mind is shown in Fig.1: we have either a single mode STS evolving in a lossy channel with parameter Γ followed by a measurement at the output, or a two-mode STS with the damping process occurring on one of the two modes, followed by a measurement on both of the modes.

The propagation of a mode of radiation in a lossy channel corresponds to the coupling of the mode a with a zero temperature reservoir made of large number of external modes. By assuming a Markovian reservoir and weak coupling between the system and the reservoir the dynamics of the system is described by the Lindblad Master equation [33]

$$\dot{\rho} = \frac{\Gamma}{2} \mathcal{L}[a]\rho \quad (27)$$

where $\mathcal{L}[a]\rho = 2a\rho a^\dagger - a^\dagger a\rho - \rho a^\dagger a$. The general solution of Eq. (27) may be expressed with the operator-sum representation of the associated CP-map i.e., upon writing $\eta = e^{-\Gamma t}$

$$\varrho(\eta) = \sum_m V_m \varrho V_m^\dagger$$

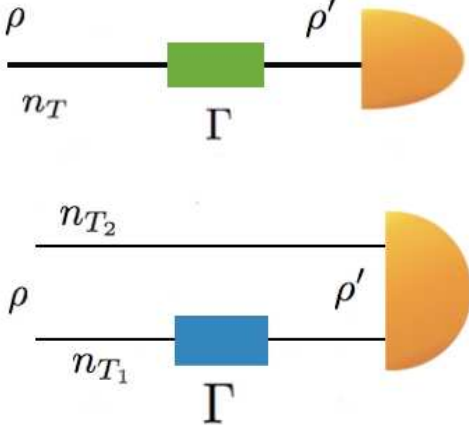


FIG. 1: Single- and two-mode schemes for the discrimination of lossy channels. Top: a single mode Gaussian state enters in a lossy channel with damping rate Γ and then a measurement apparatus detect the output signal ρ' . Bottom: the lossy channel acts on a mode of a bipartite two-mode squeezed thermal state ρ and then the final state ρ' is measured.

where

$$V_m = \sqrt{\frac{(1-\eta)^m}{m!}} a^m \eta^{\frac{1}{2}(a^\dagger a - m)},$$

and ϱ is the initial state.

A. Single-mode case

Let us now start with single-mode states. Eq. (27) can be recast into a Fokker-Planck equation for the Wigner function in terms of the quadrature variables q and p ,

$$\dot{W} = \frac{\Gamma}{2} [\partial_{\mathbf{X}}^T \mathbf{X} + \partial_{\mathbf{X}}^T \boldsymbol{\sigma}_\infty \partial_{\mathbf{X}}^T] W \quad (28)$$

where $\mathbf{X} = (q, p)^T$, $\partial_{\mathbf{X}} = (\partial_q, \partial_p)^T$ and we introduced the diffusion matrix $\boldsymbol{\sigma}_\infty = \text{diag}(1/2, 1/2)$. Solving the equation for the Wigner function of a single-mode Gaussian states one can obtain the evolution equation for $\boldsymbol{\sigma}$

$$\dot{\boldsymbol{\sigma}} = -\Gamma(\boldsymbol{\sigma} - \boldsymbol{\sigma}_\infty) \quad (29)$$

which yields to

$$\boldsymbol{\sigma}(t) = e^{-\Gamma t} \boldsymbol{\sigma}_0 + (1 - e^{-\Gamma t}) \boldsymbol{\sigma}_\infty \quad (30)$$

which describes the evolution of an initial Gaussian state with CM $\boldsymbol{\sigma}_0$ towards the stationary state given by the Gaussian state of the environment with CM $\boldsymbol{\sigma}_\infty$. The input state we considered in the scheme of Fig. 1 is a squeezed thermal state with an average number of thermal photons given by n_T and, without loss of generality,

a real squeezing parameter r . The covariance matrix is given in Eq. (15), with

$$\begin{aligned} a &= \frac{1}{2} (1 + 2n_T) e^{2r} \\ b &= \frac{1}{2} (1 + 2n_T) e^{-2r}. \end{aligned} \quad (31)$$

The evolved CM of the single mode case, Eq. (30) reads

$$\boldsymbol{\sigma}' = e^{-\Gamma} \boldsymbol{\sigma} + (1 - e^{-\Gamma}) \boldsymbol{\sigma}_\infty = \begin{pmatrix} a_\Gamma & 0 \\ 0 & b_\Gamma \end{pmatrix}, \quad (32)$$

where from now on we omit the index of $\boldsymbol{\sigma}_0$, replace $\boldsymbol{\sigma}(t) = \boldsymbol{\sigma}'$ and, since the loss parameter always appears as Γt , consider that the time t has been absorbed in Γ . In order to compute the QCB of Eq. (25), we need the number of thermal photons n_Γ and the squeezing parameter r_Γ after the evolution in the lossy channel. Upon rewriting $\boldsymbol{\sigma}'$ in the standard form we get

$$\begin{aligned} n_\Gamma &= \sqrt{\det[\boldsymbol{\sigma}']} - 1/2 \\ r_\Gamma &= 1/4 \log \left[\frac{e^{-\Gamma} a + (1 - e^{-\Gamma}/2)}{e^{-\Gamma} b + (1 - e^{-\Gamma}/2)} \right] \end{aligned} \quad (33)$$

with

$$\begin{aligned} a_\Gamma &= \frac{1}{2} (1 + 2n_\Gamma) e^{2r_\Gamma} \\ b_\Gamma &= \frac{1}{2} (1 + 2n_\Gamma) e^{-2r_\Gamma}. \end{aligned} \quad (34)$$

The quantum Chernoff bound is then obtained from Eq. (25) with the substitutions $n \rightarrow n_T$ and $n' \rightarrow n_\Gamma$.

B. Two-mode case

The map describing the evolution of a two-mode Gaussian state according to the scheme of Fig.1 is $\mathcal{E}_\Gamma \otimes \mathbb{I}_2$. At the level of the CM it corresponds to the following transformation

$$\begin{aligned} \boldsymbol{\sigma}_\Gamma &= \left(e^{-\Gamma/2} \mathbb{I}_2 \oplus \mathbb{I}_2 \right) \boldsymbol{\sigma} \left(e^{-\Gamma/2} \mathbb{I}_2 \oplus \mathbb{I}_2 \right) \\ &+ (\mathbb{I}_4 - e^{-\Gamma} \mathbb{I}_2 \oplus \mathbb{I}_2) \boldsymbol{\sigma}_\infty \end{aligned} \quad (35)$$

where we have used the same notation introduced for the single-mode case. If the input state is a two-mode squeezed thermal state of the form $\rho_2 = S_2(r) \nu_1 \otimes \nu_2 S_2(r)^\dagger$ and CM given in Eq. (17), then also the output state belongs to the same class, with the replacements $r \rightarrow r_\Gamma$, $n_{T1} \rightarrow n_{\Gamma1}$, $n_{T2} \rightarrow n_{\Gamma2}$. The covariance matrix in Eq. (35) may be recast in the standard form as

$$\boldsymbol{\sigma}_\Gamma = \frac{1}{2} \begin{pmatrix} A_\Gamma \mathbb{I}_2 & C_\Gamma \sigma_z \\ C_\Gamma \sigma_z & B_\Gamma \mathbb{I}_2 \end{pmatrix} \quad (36)$$

and the explicit form of the parameters of the evolved state may be obtained from the very definition of the

symplectic invariants. For two-mode squeezed thermal states we have

$$\begin{aligned} A_\Gamma - B_\Gamma &= n_{1\Gamma} - n_{2\Gamma} \\ \sqrt{\det \sigma_\Gamma} &= \frac{1}{4} (2n_{1\Gamma} + 1)(2n_{2\Gamma} + 1) \\ C_\Gamma &= (n_{1\Gamma} + n_{2\Gamma} + 1) \sinh 2r_\Gamma \end{aligned} \quad (37)$$

The QCB is then obtained using Eq. (26) and the replacements $n_1 \rightarrow n_{2T}$, $n_2 \rightarrow n_{2T}$, $n'_1 \rightarrow n_{1\Gamma}$, $n'_2 \rightarrow n_{2\Gamma}$.

VI. DETECTION OF LOSSY CHANNELS

In this section we address the discrimination of lossy channels probed by single- and two-mode STS and evaluate the QCB as a function of the total energy impinged into the channel, the damping and the fraction of squeezing. In particular, we are going to focus to the case when one of the two channels is the identity, i.e. the problem of discriminating the presence of a possible damping process, leading to the output signal $\mathcal{E}_\Gamma(\rho)$ from its absence, which would leave any probe ρ unchanged. Our aim is to characterize the kind of states that give the optimal discrimination, i.e. we look for the minimum of the QCB as a function of the state parameters.

Let us denote by N_1 and N_2 the total energy (average number of photons) of a single- and two-mode state respectively. They are given by

$$N_1 = n_T + n_S + 2n_S n_T, \quad (38)$$

$$N_2 = n_{1T} + n_{2T} + 2n_S + 2n_S(n_{1T} + n_{2T}), \quad (39)$$

where n_T is the number of thermal photons for the single mode, n_{1T} and n_{2T} the corresponding quantity for the two-mode state, and $n_S = \sinh^2 r$ denote the energy due to squeezing, i.e. the energy of a single-mode squeezed vacuum. In order to analyze the effect of squeezing and to compare the performances of single- and two-mode states we introduce a different parametrization of the states, based on the total energy and the squeezing fraction, which is defined as the fraction of total energy employed in squeezing. Using Eq. (38) we have, for single-mode states

$$n_S = \beta_1 N_1 \quad (40)$$

$$n_T = \frac{(1 - \beta_1)N_1}{1 + 2\beta_1 N_1}. \quad (41)$$

For two-mode states we also introduce the parameter $0 \leq \gamma \leq 1$, denoting the fraction of the total thermal energy used for the first mode, thus arriving at

$$n_S = 2\beta_2 N_2 \quad (42)$$

$$n_{1T} = \gamma \frac{(1 - 4\beta_2)N_2}{1 + 4\beta_2 N_2} \quad (43)$$

$$n_{2T} = (1 - \gamma) \frac{(1 - 4\beta_2)N_2}{1 + 4\beta_2 N_2}. \quad (44)$$

In order to make a fair comparison between the performances of single- and two-mode probes in discriminating the channels, we will assume that they have the same total and squeezing energy, i.e.

$$\begin{aligned} N_1 &= N_2 = N, \\ \beta_1 &= 2\beta_2 = \beta \quad 0 \leq \beta \leq 1, \end{aligned} \quad (45)$$

and denote by $Q_1(N, \beta) = \min_s Q_{1s}$ the single-mode QCB and by $Q_2(N, \beta, \gamma) = \min_s Q_{2s}$ the corresponding two-mode one.

The minimum values of Q_1 and Q_2 correspond to the conditions of maximal discriminability of the two states i.e. to the optimal probes states. In both cases, the minimum is achieved for $\beta = 1$, i.e. the optimal probes are given by single- and two-mode squeezed vacuum. In this case, the input state is pure and the s-overlap in Eq. (4) is minimized for $s = 0$, so that the QCB corresponds to the fidelity between the input state and the corresponding evolved one. We have

$$Q_1(N, \beta) = \langle r | \rho_{1\Gamma} | r \rangle = \frac{1}{\sqrt{1 + N(1 - \eta^2)}} \quad (46)$$

$$Q_2(N, \beta, \gamma) = \langle \langle r | \rho_{2\Gamma} | r \rangle \rangle = f(N, \eta), \quad (47)$$

where $|r\rangle = S(r)|0\rangle$ and $|\langle r|\rangle = S_2(r)|0\rangle$ denote single- and two-mode squeezed vacuum, $\rho_{1\Gamma} = \mathcal{E}_\Gamma(|r\rangle\langle r|)$, $\rho_{2\Gamma} = \mathcal{E}_\Gamma(|\langle r|\rangle\langle\langle r|)$ the corresponding evolved states, and we have introduced the symbol $\eta = e^{-\Gamma}$ to denote the damping of the channel. The expression of the function $f(N, \eta)$ is cumbersome and it will be not reported here. It is a decreasing function of N and an increasing function of η (larger Γ makes the discrimination easier) and, as expected, it is independent on γ .

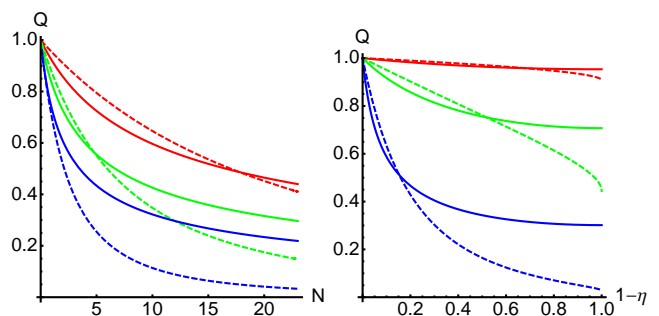


FIG. 2: (Left): single mode (solid lines) and two mode (dashed line) QCB for fixed $\beta = 1$ and different losses as a function of the energy N . From top to bottom $\Gamma = 0.1, 0.3, 1$ (red, green and blue lines respectively) (Right): single mode (solid lines) and two mode (dashed line) QCB for fixed $\beta = 1$ as a function of $1 - \eta$. From top to bottom $N = 0.1, 1, 10$ (red, green and blue lines respectively).

This behavior is illustrated in the left panel of Fig. 2, which shows that discrimination is improved by increasing the probe energy N . As expected, for larger values of Γ the discrimination is easier and the QCB smaller. The behavior of Q against the damping Γ for different values

of the probe energy is illustrated in the right panel of Fig. 2 where we show Q_1 and Q_2 as a function of $1 - \eta$.

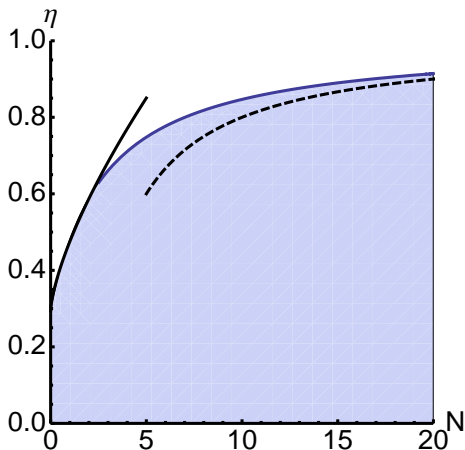


FIG. 3: The filled area indicates the values of the probe energy N and the absorption η for which, in the pure probe case ($\beta = 1$), the two-mode states lead to a smaller value of the QCB compared to single-mode ones. The solid and the dashed lines denotes the behavior of the threshold η_t for small and large N respectively.

For any value of the damping rate smaller than a critical value $\Gamma < \Gamma_c$ there is a threshold on the probe energy that makes two-mode probes more convenient than the corresponding single-mode ones. This threshold decreases for increasing values of Γ and for damping larger than the critical value $\Gamma > \Gamma_c$ two-mode probes are always better than single-mode ones independently on their energy. We have numerically evaluated the critical value $\Gamma_c \simeq 1.22$, corresponding to $\eta_c \simeq 0.3$. This phenomenon is illustrated in Fig. 3, where we show, in the $N - \eta$ plane, the region where the two-mode probes are convenient. In terms of η the threshold increases with the probe energy N ; we have that $\eta_c = \eta_t$ for $N = 0$, $\eta_t \simeq \eta_c + 0.18 N^{0.7}$ for small N (the solid line) and $\eta_t \simeq 1 - 2/N$ for large N (dashed line).

It should be said that in realistic conditions it is unlikely to have pure squeezed vacuum employable as probe states for channel discrimination. Therefore, the investigation of the performances of squeezed thermal states is in order. In this case the two-mode QCB Q_2 also depends on the parameter γ , which quantifies the fraction of thermal photons for each mode. We remind that for $\beta = 1$ the thermal energy is zero and therefore the quantum Chernoff bound does not depend on γ . The minimum of Q_2 is achieved for $\gamma = 1$, i.e.

$$n_{T_1} = \frac{(1 - \beta)N}{1 + 2\beta N} \quad n_{T_2} = 0.$$

This means that discrimination is easier when all the thermal photons are in the dissipative channel. In this case the two-mode probes are more effective than single-mode one independently of the absorption parameter, the

energy and the fraction of squeezing, i.e. $Q_2(N, \beta, 1) < Q_1(N, \beta) \forall N, \forall \beta$, and $\forall \Gamma$. In other words, in realistic conditions of interest for experimental implementations two-mode probes always perform better than single-mode ones.

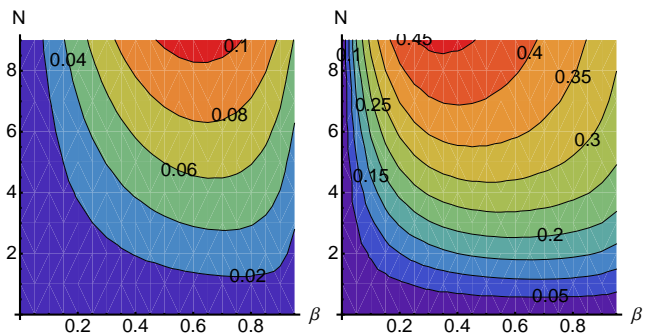


FIG. 4: (Color online) Density plot of the QCB reduction ΔQ as function of the squeezing fraction β and the probe energy N . The left plot is for $\Gamma = 0.1$ and the right one for $\Gamma = 0.9$.

In order to quantify the improvement we introduce the QCB reduction ΔQ as

$$\Delta Q = Q_1(N, \beta) - Q_2(N, \beta, 1). \quad (48)$$

We have $\Delta Q > 0$ whenever the two-mode probes are more convenient than single-mode ones and $\Delta Q < 0$ in the opposite case. In Fig. 4 we show the behavior of ΔQ as function of the squeezing fraction and the probe energy for two different values of the damping. As it is apparent from the density plot the QCB reduction increases with the damping itself and with energy, whereas it shows a minimum for intermediate values of the squeezing fraction.

As mentioned above, for $\gamma = 1$ two-mode probes are more effective than single-mode one independently on the values of N , β and Γ . In addition, the relation $Q_2(N, \beta, \gamma) < Q_1(N, \beta)$ is robust against fluctuations of γ around the optimal value $\gamma = 1$, i.e. it holds approximately also for $\gamma \lesssim 1$. This fact is of course relevant for possible implementations and it is illustrated in Fig. 5 where we report the QCB reduction

$$\Delta Q_\gamma = Q_1(N, \beta) - Q_2(N, \beta, \gamma),$$

for a sample of STS (10^3 states) with random values of N , β , and Γ and different values of γ . As it is apparent from the plot most of the states leads to positive ΔQ also for γ quite different from unity.

VII. QCB AND QUANTUM CORRELATIONS

Since two-mode probes are always convenient for $\beta \neq 1$ and $\gamma = 1$, a natural question arises on whether this improvement should be ascribed to some kind of correlations, either classical or quantum, as, for example, those

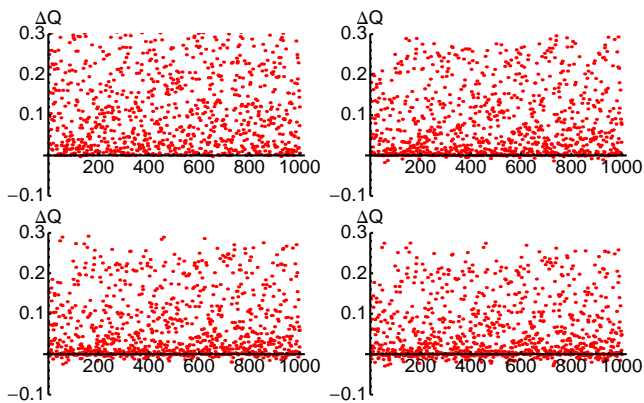


FIG. 5: (Color online) QCB reduction for a sample of STS with random values of N , β , and Γ and different values of γ (top left $\gamma = 0.99$, top right $\gamma = 0.9$, bottom left $\gamma = 0.8$, bottom right $\gamma = 0.7$)

quantified by entanglement, quantum discord or quantum mutual information.

In order to quantify the degree of entanglement of a two-mode Gaussian state, it is suitable to use the logarithmic negativity that is defined as

$$E = \max\{0, -\log 2\tilde{d}_-\} \quad (49)$$

where \tilde{d}_- is the smallest symplectic eigenvalue of the partially transposed state, i.e.

$$\tilde{d}_-^2 = \frac{1}{2}[\tilde{\Delta} - \sqrt{\tilde{\Delta}^2 - 4I_4}] \quad (50)$$

where $\tilde{\Delta} = I_1 + I_2 - 2I_3$. The quantum discord has been defined as the mismatch of two different quantum analogues of classically equivalent expression of the mutual information. For a bipartite STS with CM as in Eq. (17) the quantum discord may be written as [28]

$$D = h(\sqrt{I_2}) - h(d_-) - h(d_+) + h\left(\frac{\sqrt{I_1} + 2\sqrt{I_1 I_2} + 2I_3}{1 + 2\sqrt{I_2}}\right) \quad (51)$$

where $h(x) = (x + \frac{1}{2})\log(x + \frac{1}{2}) - (x - \frac{1}{2})\log(x - \frac{1}{2})$. Finally, the quantum mutual information, which quantifies the amount of total, classical plus quantum, correlations, is given by $I = S(\rho_A) + S(\rho_B) - S(\rho_{AB})$, where $S(\rho) = -\text{Tr}[\rho \log \rho]$ is the von Neumann entropy of the state ρ and $\rho_{A(B)} = \text{Tr}_{B(A)}[\rho_{AB}]$ are the partial traces over the two subsystems. For a Gaussian bipartite state in the canonical form (17) the quantum mutual information reduces to

$$I = \frac{1}{2} \left[h(\sqrt{I_1}) + h(\sqrt{I_2}) - h(d_+) - h(d_-) \right] \quad (52)$$

where the symplectic eigenvalues d_{\pm} are given in Eq. (19). A bipartite Gaussian state is entangled iff $\tilde{d}_- < 1/2$, then the logarithmic negativity gives positive values for all the entangled states and 0 otherwise. For

what concerns the discord, we have that for $0 \leq D \leq 1$ the state may be either entangled or separable, whereas all the states with $D > 1$ are entangled. All the three quantifiers are monotonically increasing functions of N and β and decreasing functions of η . Notice that for pure states the three measures are equivalent, whereas for mixed states, as in the case under investigation in this Section, they generally quantify different kind of correlations.

In the upper panels of Fig. 6 we report the QCB reduction as a function of the three correlations quantifiers, mutual information, discord and entanglement, for different values of the damping and for two values of the squeezing fraction ($\beta = 0.1$ for the left panel and $\beta = 0.9$ for the right one). As it is apparent from the plot, the QCB reduction is a monotone function of all the three quantities and this suggests that while correlations should definitely be considered a resource for channel discrimination, it is not relevant whether these correlations are classical or quantum. This is confirmed by the plots in the middle panel, which are density plots of the QCB reduction ΔQ as a function of discord and entanglement for $\Gamma = 0.2$ (left) and $\Gamma = 0.8$ (right) respectively. Notice that the behavior of the QCB reduction against the correlation quantifiers is not a result of a monotonicity of themselves each other, i.e. ΔQ is a monotonic increasing function (at fixed Γ) of both D and E but they are not a monotone function one of each other. This is shown by the lower panels of Fig. 6 where we report entanglement (left) and discord (right) as a function of the mutual information for a random sample (10^4 states) of STS. Families of states with increasing mutual information and decreasing entanglement and viceversa may be easily found.

VIII. CONCLUSIONS

In this paper we have addressed the problem of quantum discrimination of lossy channels probed by Gaussian states. In particular, we focused to the case when one of the two channels is the identity, i.e. the problem of discriminating the presence of a possible damping process from its absence. We have analyzed the use of single-mode Gaussian probe as well as the case where the channel acts on a mode of a bipartite two-mode Gaussian probe. In order to compare the two strategies we have calculated the quantum Chernoff bound in both cases, thus evaluating the upper bound for the error probability in the case of many repeated uses of the channel. We found that the optimal probes are the squeezed vacuum states for both single- and two-mode probes and that discrimination improves by increasing the total energy. The quantum Chernoff bound has a decreasing monotonic behavior as function of the absorption parameter and there is a threshold on the probe energy that makes two-mode input states more convenient than single-mode one. We have then addressed discrimination in realistic

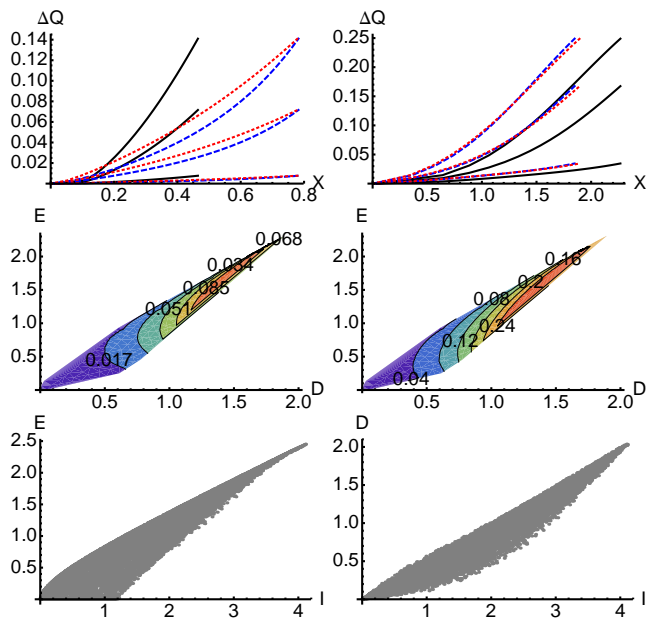


FIG. 6: (Color online) The upper panels shows the QCB reduction as a function of the three correlations quantifiers $X=I,D,E$, mutual information (dotted red), discord (dashed blue) and entanglement (solid black) for different values of the damping (from top to bottom $\Gamma = 0.9, 0.5, 0.1$ for all the three quantifiers) and for two values of the squeezing fraction ($\beta = 0.1$ for the left panel and $\beta = 0.9$ for the right one). The middle panel is made of density plots of the QCB reduction ΔQ as a function of discord and entanglement for $\Gamma = 0.2$ (left) and $\Gamma = 0.8$ (right) respectively. The lower panel reports entanglement (left) and discord (right) as a function of the mutual information for a random sample (10^4 states) of STS.

conditions, where it is unlikely to have pure squeezing, and have shown that two-mode probes always perform better than single-mode ones when all the thermal photons are directed to the dissipative channel. In addition, this result is robust against fluctuations i.e. it holds approximately also when the thermal photons are distributed in a more balanced way.

Our results show that the correlations between the subsystems of a two-mode state represent a resource for experimental implementations, and may be exploited to improve discrimination. Motivated by this finding we also investigate the role of correlations in the improvement of discrimination and found that at fixed squeezing the QCB reduction is a monotone function of the mutual information, entanglement and quantum discord. We thus conclude that correlations are a resource for channel discrimination independently of their nature, either quantum or classical.

Acknowledgments

The authors thank Marco Genoni and Stefano Olivares for useful discussions.

-
- [1] H.-P. Breuer and F. Petruccione, *The Theory of Open Quantum Systems* (Oxford University Press, Oxford, 2002).
 - [2] A. Serafini, M. G. A. Paris, F. Illuminati, and S. De Siena, *J. Opt. B* **7**, R19 (2006).
 - [3] V. D'Auria, C. de Lisio, A. Porzio, S. Solimeno, and M. G. A. Paris, *J. Phys. B* **39**, 1187 (2006).
 - [4] W. H. Zurek, *Rev. Mod. Phys.* **75**, 715 (2003).
 - [5] M. Brune, J. Bernu, C. Guerlin, S. Deléglise, C. Sayrin, S. Gleyzes, S. Kuhr, I. Dotsenko, J. M. Raimond, and S. Haroche, *Phys. Rev. Lett.* **101**, 240402 (2008); S. Deléglise, I. Dotsenko, C. Sayrin, J. Bernu, M. Brune, J. Raymond, and S. Haroche, *Nature* **455**, 510 (2008).
 - [6] C. W. Helstrom, *Quantum Detection and Estimation Theory* (Academic Press, New York, 1976).
 - [7] A. Chefles, *Contemp. Phys.* **41**, 401 (2000).
 - [8] J. A. Bergou, U. Herzog, M. Hillery in *Quantum State Estimation*, Lect. Not. Phys. **649**, J. Rehacek, M. G. A. Paris (Eds) (Springer, Berlin, 2004), pp 417-465.
 - [9] A. Chefles in *Quantum State Estimation*, Lect. Not. Phys. **649**, J. Rehacek, M. G. A. Paris (Eds) (Springer, Berlin, 2004), pp 467-511.
 - [10] V. Kargin, *Ann. Stat.* **33**, 959 (2005).
 - [11] J. Calsamiglia, R. Muñoz-Tapia, L. Masanes, A. Acín, E. Bagan, *Phys. Rev. A* **77**, 032311 (2008).
 - [12] K. M. R. Audenaert, J. Calsamiglia, R. Muñoz-Tapia, E. Bagan, L. Masanes, A. Acín, F. Verstraete, *Phys. Rev. Lett.* **98**, 160501 (2007).
 - [13] S. Pirandola and S. Lloyd, *Phys. Rev. A* **78**, 012331 (2008).
 - [14] M. Boca, I. Ghiu, P. Marian, and T. A. Marian, *Phys. Rev. A* **79**, 014302 (2009).
 - [15] I. Ghiu, G. Björk, P. Marian, and T. A. Marian, *Phys. Rev. A* **82**, 033823 (2010).
 - [16] D. Abasto, N. T. Jacobson, and P. Zanardi, *Phys. Rev. A* **77**, 022327 (2008).
 - [17] C. Invernizzi and M. G. A. Paris, *J. Mod. Opt.* **57**, 1362 (2010).
 - [18] A. Ferraro, S. Olivares, M. G. A. Paris, *Gaussian States in Quantum Information* (Bibliopolis, Napoli 2005).
 - [19] S. L. Braunstein and A. K. Pati, *Quantum Information Theory with Continuous Variables* (Kluwer Academic, Dordrecht, 2003).
 - [20] V. D'Auria, S. Fornaro, A. Porzio, S. Solimeno, S. Olivares, and M. G. A. Paris, *Phys. Rev. Lett.* **102**, 020502 (2009).

- [21] G. Adesso, F. Dell'Anno, S. De Siena, F. Illuminati, and L. A. M. Souza, Phys. Rev. A **79**, 040305(R) (2009).
- [22] H. Venzl and M. Freyberger, Phys. Rev. A **75**, 042322 (2007).
- [23] A. Monras, M. G. A. Paris, Phys. Rev. Lett. **98**, 160401 (2007).
- [24] A. Monras and F. Illuminati, Phys. Rev. A **81**, 062326 (2010); A. Monras and F. Illuminati arXiv:1010.0442.
- [25] H. Ollivier and W. Zurek, Phys. Rev. Lett. **88**, 017901 (2001); W. Zurek, Phys. Rev. A **67**, 012320 (2003).
- [26] C. A. Rodriguez-Rosario, K. Modi, A. Kuah, A. Shaji, and E. C. G. Sudarshan, J. Phys. A **41**, 205301 (2008); M. Piani, P. Horodecki, and R. Horodecki, Phys. Rev. Lett. **100**, 090502 (2008).
- [27] A. Ferraro, L. Aolita, D. Cavalcanti, F. M. Cucchietti, and A. Acin, Phys. Rev. A **81**, 052318 (2010).
- [28] P. Giorda and M. G. A. Paris, Phys. Rev. Lett. **105**, 020503 (2010); G. Adesso and A. Datta, Phys. Rev. Lett. **105**, 030501 (2010).
- [29] V. Vedral, Rev. Mod. Phys. **74**, 197 (2002).
- [30] M. Nussbaum and A. Szkola, Ann. Stat. **37**, 1040 (2009).
- [31] C.A. Fuchs and J. V. de Graafs, IEEE Trans. Inf. Theory **45**, 1216 (1999).
- [32] A. Serafini, F. Illuminati, and S. de Siena, J. Phys. B **37**, L21 (2004).
- [33] D. F. Walls and G. J. Milburn, *Quantum Optics* (Springer, Berlin, 1994).